

Ionization mechanisms near three-photon resonances in Xe-Ar and Xe-Kr mixtures

M. G. Payne, W. R. Ferrell, and W. R. Garrett

*Chemical Physics Section, Health and Safety Research Division, Oak Ridge National Laboratory,
Oak Ridge, Tennessee 37830*

(Received 22 November 1982)

Unfocused linear polarized laser light is used to explore ionization mechanisms in the region near three-photon resonances in Xe. In Xe-Ar and Xe-Kr mixtures at elevated concentrations, processes involving dimer absorption of third-harmonic photons are shown to play an important role in determining ionization yields, and a method for using the observed ionization to measure vacuum ultraviolet absorption is described.

I. INTRODUCTION

The multiphoton ionization of Xe at concentrations above $10^{15}/\text{cm}^3$ has recently been of considerable interest.¹⁻⁸ The first study by Aaron and Johnson¹ was carried out for $N_{\text{Xe}} > 10^{18}/\text{cm}^3$. At such elevated concentrations the expected enhancement in ionization at $\lambda=440.88$ nm due to the three-photon resonance between the ground state and the $6s$ ($J=1$) state was completely absent. This was particularly surprising since the nearby ($\lambda=440.26$ nm) four-photon resonance enhancement with the $4f$ ($J=2$) state was very large.

More recently Miller *et al.*² showed that the 440.88-nm resonant enhancement is easily observed at low concentrations and is larger than the four-photon resonance signal at 440.26 nm. However, when N_{Xe} was increased to $\sim 3 \times 10^{16}/\text{cm}^3$ the 440.26-nm signal remained while the 440.88-nm resonance was not observable.

Payne and Garrett³ suggested that a self-consistent theory of ionization near the photon resonances at elevated concentrations must allow for the presence of a third-harmonic field (which has a resonantly enhanced nonlinear susceptibility) and allow the atom to simultaneously interact nonlinearly with the laser field and linearly with the radiation field due to the other atoms. The latter theory predicted the disappearance of resonance associated with odd-photon resonances at elevated concentrations and, in particular, predicted the qualitative observations that had been made on Xe.

Additional predictions of the theory suggested that an ionization signal would be observed for focused beams on the high energy side of a three-photon resonance and that the line shape would be very similar to the phase-matching curve for third-harmonic generation (THG). The latter signal arises because of processes involving the absorption of a third-harmonic photon plus other photons to ionize.

The latter process is easily shown to be orders of magnitude more effective near 440.88 nm in Xe than five-photon ionization by the laser.

The initial theory was appropriate to $N_{\text{Xe}} \leq 3 \times 10^{15}/\text{cm}^3$ due to some approximations on the indices of refraction, and it dealt only crudely with the geometry of focused laser beams. More recent theoretical work⁴⁻⁶ has dealt more carefully with the geometry, has removed some of the restrictions on concentration, and gives additional physical insight into the mechanism for the suppression of odd-photon resonances.

It is found that as the three-photon resonance is approached the third-harmonic field decrease due to very large phase mismatches associated with the sharp changes in index of refraction at 3ω , and due to scattering and absorption in the region near the resonance. However, it remains large enough so that its amplitude gives rise to a one-photon Rabi frequency which is equal to the three-photon Rabi frequency due to the laser. (These quantities are related because the three-photon resonance also dominates the nonlinear response.) In calculations of the atomic response the interaction with the two fields occurs coherently and one term is 180° out of phase with the other. Thus, once the phase-matching region no longer overlaps with the laser linewidth there is a very complete cancellation in the overall pumping of the upper level. The cancellation includes not only the linewidth of the level, but also any enhancement of multiphoton ionization involving photons on the near wing of the resonance.

II. RELEVANT THEORETICAL AND EXPERIMENTAL STUDIES

Glowia and Sander⁷ have recently confirmed the involvement of the third-harmonic signal in the suppression of the 440.88-nm resonance in Xe by pointing out that with circularly polarized light no

THG occurs. However, with counterpropagating circularly polarized beams, three-photon transitions with $\Delta J = 1$ can occur by the absorption of one photon from one beam and two from the beam with the opposite direction of propagation. Thus, they demonstrated with the latter arrangement that a strong signal was observed at three-photon resonance, while with even higher laser power densities and linearly polarized light no resonance was observed in the absence of a counterpropagating beam.

Jackson and Wynne⁸ extended studies with counterpropagating beams to linearly polarized beams, and again found the three-photon resonance which was absent without the counterpropagating beam being present. Both of the above studies were carried out with focused beams.

In a longer paper on focused beams⁴ some of us have pointed out that with counterpropagating plane polarized beams, parts of the three-photon transition amplitude due to absorbing three photons with the same direction of propagation are still coherently canceled by parts of a one-photon amplitude associated with the interaction of the atom with the third-harmonic field propagating in the same direction. However, the three-photon interaction with the laser fields also involves processes in which two photons are absorbed from one beam and one photon is absorbed from the beam with opposite direction of propagation. This part of the nonlinear interaction with the laser fields has no corresponding third-harmonic field to cancel it, and a substantial part of the resonance signal remains.

Until recently there has been a lack of really quantitative measurements related to the suppression of the laser pumping of odd-photon resonances. Part of the difficulty is due to small ionization signals. Thus, gas amplification has been required in order to make the observations, and the gain of the amplification used in the detection process changes with concentration. It has, therefore, not been possible to measure absolute ionization signals as a function of pressure. In addition, most of the work has been carried out with focused laser beams with nondiffraction-limited beam divergences. With such lasers it is difficult to account simultaneously for the power densities near focus and the effects of phase matching. In addition, if counterpropagating beams are used it is difficult to achieve and maintain good beam overlap in the region of highest power densities.

We have recently submitted back-to-back papers^{6,9} in which, for the first time, theory has been compared in some detail with experiment. The theory⁶ deals in detail with the ionization produced when a linearly polarized broad bandwidth laser having a Gaussian radial intensity profile of beam

waist d is passed unfocused through a length L of gaseous medium. The line shape of the laser is taken to be $\propto \exp[-(\omega - \bar{\omega})^2/2\sigma^2]$ and the broad bandwidth effects are dealt with via a chaotic field model which yields the preceding line shape.

Experimentally⁹ an unfocused linearly polarized laser beam with $d = 0.05$ cm, $\sigma \approx 9.3 \times 10^{10}$ /sec the pulse length $\tau = 1.7 \times 10^{-8}$ sec, and ϵ as the energy per pulse $\approx 1-5$ mJ was used to verify the theoretical predictions. The same laser is used in the present study. The cell (also used in the present study) containing the sample has guard rings which kept ionization produced within 3.8 cm of the input and output windows from being observed. The laser beam's angle of incidence on the cell windows deviated from the normal sufficiently so that reflections from the back windows were completely separated from the incident beam in the 11.5-cm region between the guard rings where the ionization signal was observed.

With $N_{Xe} > 6 \times 10^{16}/\text{cm}^3$ (or with N_{Xe} much smaller if Kr was used as a buffer gas), a ⁵⁵Fe x-ray source could be used to calibrate the gain associated with the gas amplification. Thus, over an extremely large range of N_{Xe} absolute determinations could be made of the ionization signal. The ⁵⁵Fe x rays entered the cell through a Be window, and the source could be removed during data collection.

Theory predicts that with the use of a laser of the characteristics described above, with the cell described previously,⁹ and without a counterpropagating beam, the 440.88-nm resonance in Xe will be strongly suppressed for $N_{Xe} > 10^{13}/\text{cm}^3$. Experimentally, without a counterpropagating beam no signal could be observed for any $N_{Xe} > 3 \times 10^{13}/\text{cm}^3$. However, with 50% of the incident beam reflected back through the cell a signal was observed which at $\epsilon = 5$ mJ and $N_{Xe} = 3 \times 10^{13}/\text{cm}^3$ was ≈ 20 electrons. This signal was found to grow linearly with N_{Xe} reaching ~ 20000 electrons at $N_{Xe} = 3 \times 10^{16}/\text{cm}^3$. It was also established⁹ that the resonant ionization signal with counterpropagating beams was independent of Ar or Kr concentration for N_B the concentration of buffer gas $< 10^{19}/\text{cm}^3$. With smaller bandwidths, however, it is likely that strong effects due to the buffer gas would be observed by $N_B = 10^{19}/\text{cm}^3$.

A separate study showed that when F is the fraction of incident beam reflected (with perfect overlap) back through the cell and the condition $F < 0.2$ was satisfied, then the number of ions produced was proportional to F , as expected from theory. When $N_{Xe} = 0.5 \times 10^{16}/\text{cm}^3$ and $F = 0.1$, a signal of $\sim 10^4$ electrons is observed and no signal was seen with $F = 0$. This means that with the existing noise level the $F = 0$ signal was at least 200 times smaller than

that observed with $F=0.1$. Theory⁶ predicts that with the power densities and bandwidths used in the experiment a rate equation analysis of the resonance is appropriate and that the total rate of excitation of the three-photon resonance state for $N_{Xe} > 3 \times 10^{13}/\text{cm}^3$ is ($3\omega = \omega_r$ and ω_r is the resonance frequency)

$$R_\omega = \sqrt{2/3} \pi^{3/2} N_{Xe} L d^2 (F + F^2) \frac{|\bar{\Omega}(0, t)|^2}{\sigma}, \quad (1)$$

where $\bar{\Omega}_3(0, t)$ is the three-photon Rabi frequency $\Omega_3(\rho, t)$ of the transition evaluated at the mean power density for time t and at $\rho=0$, where ρ is the radial distance from the z axis which is directed along the laser beam.

In the previous experimental study⁹ it was shown that by using a buffer gas, phase matching could be achieved for various detunings of the laser to the high energy side of a three-photon resonance. With an unfocused beam it is well known¹⁰ that this occurs when

$$\Delta k \equiv \frac{3\omega}{c} [n(\omega) - n(3\omega)] = 0,$$

where $n(\omega)$ is the index of refraction of the medium at the laser frequency and $n(3\omega)$ is the index of refraction at the third-harmonic frequency. This is just the condition for constructive interference between the 3ω signal being generated by an atom at any point and the signal being generated by atoms at all other points upstream in the laser beam. It is also known that when N_{Xe} and N_B (where N_B is the buffer-gas concentration) are both increased with N_{Xe}/N_B held constant, the wavelength region over which THG occurs narrows.

When a strong one-photon resonance exists near 3ω and $P_B \gg P_{Xe}$, we can take the index of refraction for Xe to be $n_{Xe}(3\omega) \approx \kappa/\Delta_0$, where $\Delta_0 = 3\omega - \omega_r$, ω_r is the resonant frequency, and

$$\kappa = \pi N_{Xe} (e^2/m_c c) F_{01}. \quad (2)$$

In κ the quantity F_{01} is the ground-to-resonance-state oscillator strength which is 0.28 for $5p^6 1S_0 \rightarrow 5p^5 6s^2 P_{3/2}$ ($J=1$) and 0.19 for $5p^6 \rightarrow 5p^5 6s^2 P_{1/2}$ ($J=1$). If $n_B(\omega)$ and $n_B(3\omega)$ are the indices of refraction at ω and 3ω due to the buffer gas, and the buffer gas has no nearby resonances, we can take each of these to be constant in the region near the particular resonance and $(3\omega/c)[n_B(\omega) - n_B(3\omega)] \approx \Delta k_R$. Thus, Δk has the simple representation $\Delta k = \kappa/\Delta_0 + \Delta k_R$, where Δk_R is independent of Δ_0 for a particular resonance and $\Delta k_R \propto N_B$. If $n_B(3\omega)$ and $n_B(\omega)$ are known, Δk_R is easily determined. The point of optimal phase

matching occurs when $\Delta k = 0$ or $\Delta_0 = -\kappa/\Delta k_R$. Since $\kappa \propto P_{Xe}$ and $\Delta k_R \propto P_B$ we see that the detuning $\Delta\lambda$ (nm) of the laser from three-photon resonance satisfies $\Delta\lambda$ (nm) = $K_1 P_{Xe}/P_B$ at phase matching. Correspondingly, by changing the ratio of P_{Xe} to P_B one can vary $\Delta\lambda$ over a sizable range of wavelengths on the high energy side of the resonance.

In Ref. 9 it was demonstrated that with counter-propagating beams, the only significant ionization signals observed were at three-photon resonance or in a relatively narrow wavelength region about the point where phase matching occurred. This showed that on the wing of the atomic resonance line, processes involving the absorption of a third-harmonic photon dominate multiphoton ionization signals. It was suggested^{6,9} on the basis of absorption measurements by Castex¹¹ that the absorption of third-harmonic light by dimers with repulsive upper states, followed by ionization of the resulting resonance state, should be the dominant mechanism for producing ionization in the phase-matched region.

The mechanism described by Castex¹¹ gives an absorption coefficient 2β of the form

$$2\beta = K(3\omega, T) P_{Xe} P_B$$

for a situation where the buffer-gas pressure P_B is very large compared with P_{Xe} . The purpose of the present paper is to present further verification of the theory in Ref. 6 and to give a rather complete verification of the mechanisms for ionization⁶ on the blue wing of the three-photon resonance at concentrations $N_{Xe} > 3 \times 10^{15}/\text{cm}^3$ and power densities $\leq 10^8$ W/cm².

III. COMPARISON BETWEEN THEORY AND EXPERIMENT

If the description of Ref. 6 is correct, wherein the dominant ionization mechanism in the frequency region near phase matching is the absorption of third-harmonic photons by dimers followed by ionization out of the resulting resonance state sometime later in the laser pulse, then we can write an analytic expression for the expected ionization signals. Thus, from Ref. 6 we note that if R is the ratio of the peak height of the ionization at phase matching to the peak height of the ionization at three-photon resonance, then for a fraction F of the incident beam reflected back through the proportional counter (with counter volume extending from Z_1 to Z_2) in a mixture in which the laser frequency at phase matching is ω_m (with ω_r the resonance angular frequency), we can write

$$R = \left[\frac{2}{3\pi} \right]^{1/2} \left[\frac{\Delta_m^2}{\kappa L \sigma} \right] \left[\frac{1+F^3}{F+F^2} \right] \times \frac{\gamma_I(\Delta\lambda)}{\gamma_I(0)} G_1(Y_2, Y_1, \Gamma_1, 0). \quad (3)$$

Here $\Delta_m = 3\omega_m - \omega_r$, $\gamma_I(\Delta\lambda)$ is the ionization rate of the resonance state when the laser is tuned to the phase-matched frequency ω_m , and $\gamma_I(0)$ is the ionization rate of the resonance state when the laser is tuned to the three-photon resonance. Also, the

$$G_1(Y, 0, \Gamma_1, \delta_1) = \int_0^Y du e^{-u^2} \cos(\delta_1 u) \left[(Y-u)e^{-\Gamma_1 u} - \frac{1}{2\Gamma_1} (e^{-\Gamma_1 u} - e^{-\Gamma_1(2Y-u)}) \right]. \quad (5)$$

Here $\delta_1 = \sqrt{2/3}(\delta/\sigma)$, $\Gamma_1 = \sqrt{2/3}(\beta\Delta_m^2/\kappa\sigma)$, and 2β is the absorption coefficient at 3ω .

In our case $Y_2 = \sqrt{3/2}\sigma(\kappa Z_2/\Delta_m^2)$ and $Y_1 = \sqrt{3/2}\sigma(\kappa Z_1/\Delta_m^2)$, with $Z_1 = 3.8$ cm and $Z_2 - Z_1 = 11.5$ cm. This analysis is only appropriate when $(3\omega/c) |n_B(\omega) - n_B(3\omega)| L \gg 1$. Also, $\delta/\Delta_m \ll 1$ with n_B representing the contribution to the index of refraction due to the buffer gas. The line shape of the observed ionization signal in the phase-matched region is given by $G_1(Y_2, Y_1, \Gamma_1, \delta_1)$. In a few limiting cases $G_1(Y_2, Y_1, \Gamma_1, \delta_1)$ has a simple approximate form. For instance, if $Y \ll 1$ and $\beta Z_2 \ll 1$, we obtain

$$G_1(Y, 0, \Gamma_1, \delta_1) = (2\Gamma_1/\delta_1^2) [Y - \sin(\delta_1 Y)/\delta_1]. \quad (6a)$$

In this limit if P_{Xe}/P_B is held fixed and P_{Xe} is increased, the THG increases proportional to N_{Xe}^2 and the width of the phase-matched region decreases proportional to $1/N_{Xe}$. The wavelength for phase matching stays fixed. In this limit the conventional

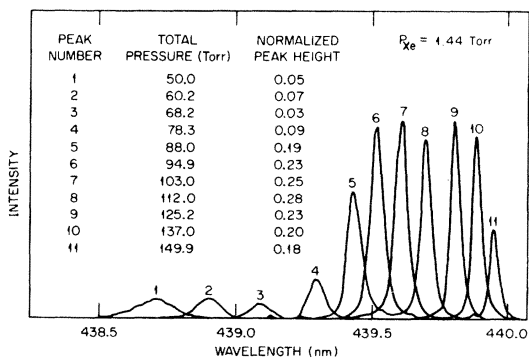


FIG. 1. Typical ionization signals observed when $P_{Xe} = 1.44$ Torr for various partial pressures of P_{Ar} . The resonance signal is not shown, but the ratio of the phase-matched peak to the resonance signal for different buffer-gas pressures is tabulated.

counting volume extends from Z_1 to Z_2 , with $L = Z_2 - Z_1$, and the reduced variable $Y = Y(Z) = \sqrt{3/2}(\kappa\sigma/\Delta_m^2)Z$. The quantities κ and F_{01} were defined previously. Finally, in terms of these variables, the quantity G_1 is defined at detuning $\delta = (3\omega - \omega_r) - \Delta_m$ (i.e., δ is the detuning in 3ω from the phase-matching frequency)

$$G_1(Y_2, Y_1, \Gamma_1, \delta_1) = G_1(Y_2, 0, \Gamma_1, \delta_1) - G_1(Y_1, 0, \Gamma_1, \delta_1), \quad (4)$$

where

theory of THG (Ref. 11) applies since $Y_2 \ll 1$, while $Y_1 > 1$ signals the onset of coherence length effects.

When phase matching occurs in a region of very low absorption, we can have $Y \gg 1$ and $\beta Z \ll 1$. For $|\delta_1| < 5$,

$$G_1(Y, 0, \Gamma_1, \delta_1) = \frac{\sqrt{\pi}}{2} Y^2 \Gamma_1 \exp(-\delta^2/6\sigma^2). \quad (6b)$$

In this limit of large N_{Xe} , but small absorption, the linewidth of the ionization signal in the phase-matched region is identical to the width observed at three-photon resonance with the counterpropagating beams. Thus, if Δ_m corresponds to a region of very low absorption and P_{Xe}/P_B is held fixed (so that Δ_m is fixed) while P_{Xe} is increased from a value where $Y_2 \ll 1$ to values where $Y_2 \gg 1$, the ionization signal at $\delta_1 = 0$ will initially increase as P_{Xe}^4 [i.e., Eq. (5)

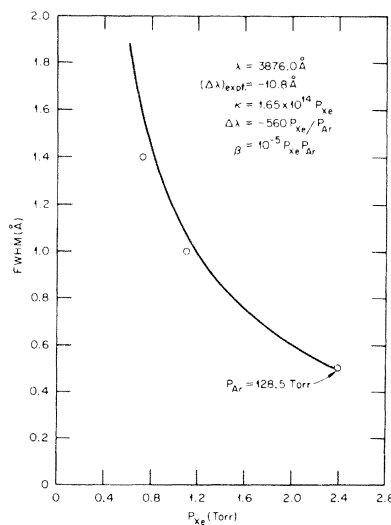


FIG. 2. Width of phase-matched ionization signal vs P_{Xe} for Xe-Ar mixtures and $\Delta\lambda = -1.08$ nm.

applies] and the ratio of this signal to the counter-propagating resonance signal is proportional to P_{Xe}^3 . However, as $Y_2 \rightarrow 1$ the linewidth of the ionization signal approaches that of the three-photon resonantly enhanced signal and the ratio of signals changes from a P_{Xe}^3 dependence over to P_{Xe}^2 dependence on Xe pressure.

$$G_1(Y, 0, \Gamma_1, \delta_1) = \frac{\Gamma_1^2}{\delta_1^2 + \Gamma_1^2} \left[Y - \frac{1}{2\Gamma_1} e^{-2\Gamma_1 Y} + \frac{2e^{-\Gamma_1 Y}}{\Gamma_1^2 + \delta_1^2} [\Gamma_1 \cos(Y\delta_1) - \delta_1 \sin(Y\delta_1)] \right]. \quad (7)$$

If $\beta Z_2 \gg 1$ and $\Gamma_1 \gg Y_2$, Eq. (5) reduces to

$$G_1(Y, 0, \Gamma_1, \delta_1) = \frac{\Gamma_1 Y}{\delta_1^2 + \Gamma_1^2}. \quad (8)$$

Before presenting data which support Eqs. (2) and (4) we will discuss qualitatively what should be observed. Suppose we begin with a gas mixture in which $P_B \gg P_{Xe}$, but with $P_{Xe} > 10$ Torr. Suppose further that the detuning in 3ω for phase matching is $\Delta_m < 3 \times 10^{13}$ /sec. If $\sigma \approx 10^{11}$ /sec and $Z_2 \approx 15.3$ cm, then initially $Y_2 > 3$ for a resonance with $F_{01} > 0.2$. If Δ_m corresponds to a region of very low absorption (i.e., $\beta L < 1$ at the initial filling of the cell), the full width of half maximum (FWHM) of the ionization signal near phase matching will be very close to the FWHM of the ionization signal observed with counterpropagating beams at three-photon resonance [i.e., Eq. (6) applies]. If the total pressure in the cell is lowered by pumping out some of the gas, then P_{Xe}/P_B remains fixed, as does the laser wavelength for phase matching. When the pressure is lowered to a point where $Y_2 \approx 1$, the FWHM of the ionization signal near phase match-

ing will have broadened slightly and the ratio of peak height of ionization signal at phase matching to that at three-photon resonance will have decreased proportionally to P_{Xe}^2 . When the cell is pumped down so that $Y_2 < 0.5$, Eq. (5) begins to apply. If $Y < 0.5$ and $Z_2 = 4Z_1$, we have $Y_1 \approx 0.25Y_2$, and the value of the FWHM in 3ω of the ionization signal at phase matching is $\approx 7.33\Delta_m^2/\kappa Z_2$, in angular frequency units.

Thus, a measure of FWHM determines $\Delta_m^2/\kappa Z_2$, while a measure of Δ_m (from the 3ω at which phase matching occurs) determines $\kappa/\Delta k_R$. Therefore if Δ_m , P_{Xe} , P_B , and FWHM are measured accurately in the region where the ratio of the peak signals is directly proportional to P_{Xe}^3 and the FWHM to $1/P_{Xe}$, one obtains an accurate measurement of κ (and therefore F_{01}) and $\Delta k_R = (3\omega/c) \times [n_B(\omega) - n_B(3\omega)]$.

A more commonly occurring limit is one in which the absorption is large or σ is smaller. In either case if the cell is filled to high pressure (assume $P_{Xe}/P_B \ll 1$) and data are collected for different P_{Xe} as the cell is pumped down, we find at fixed

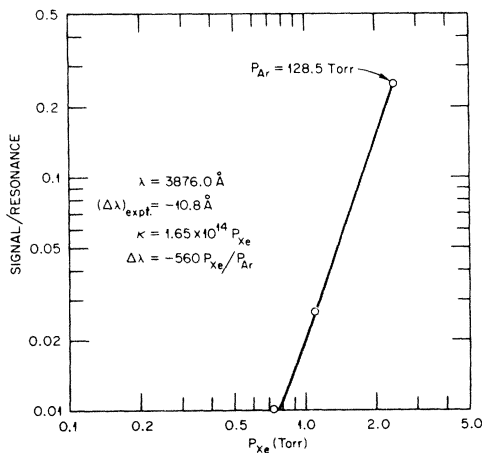


FIG. 3. Ratio of phase-matched ionization signal to three-photon resonance signal vs P_{Xe} for Xe-Ar mixtures and $\Delta\lambda = -1.08$ nm relative to the $6s'$ ($J = 1$) resonance.

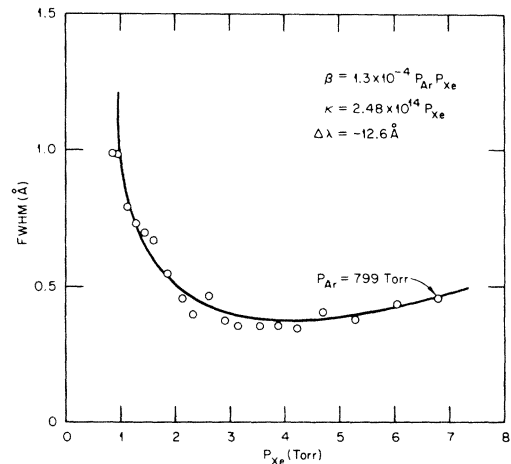


FIG. 4. Width of phase-matched ionization signal vs P_{Xe} for Xe-Ar mixtures and $\Delta\lambda = -1.26$ nm relative to the $6s$ ($J = 1$) resonance in Xe.

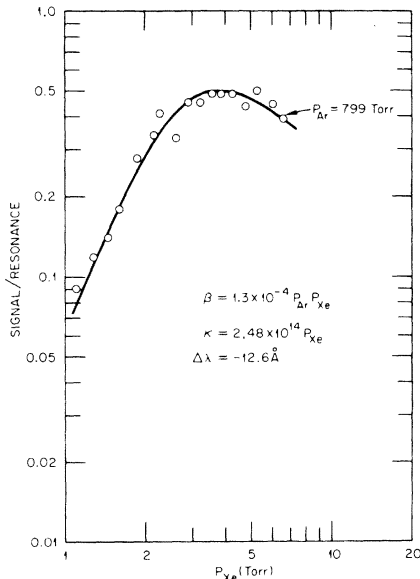


FIG. 5. Ratio of the phase-matched ionization signal to the three-photon resonance signal vs P_{Xe} for Xe-Ar mixtures and $\Delta\lambda = -1.26$ nm relative to the $6s$ ($J=1$) resonance.

P_{Xe}/P_B that $\Gamma_1 \propto P_{Xe}$ and $Y_2 \propto P_{Xe}$ with $\Gamma_1 \gg Y_2$ at all P_{Xe} . In this limit $G_1(Y, 0, \Gamma_1, \delta_1)$ is given accurately by Eq. (7). Thus, using Eqs. (2), (3), and (7) both R and the FWHM of the ionization signal near phase matching should be predicted accurately for all P_{Xe} . In this limit when $\beta Z_2 \ll 1$ and $Y_2 < 0.5$, Eq. (7) reduces to Eq. (6a) and $R \propto P_{Xe}^3$; FWHM is $\approx 7.33(\Delta_m^2/\kappa Z_2)$ and $\Delta_m = \kappa/\Delta k_R$. Again, measurements in the $Y_2 < 0.5$ region yield κ and Δk_R . However, behavior for $Y_2 > 1$ is very different than the low absorption case. When $\beta L = 2.6$ we still have $Y_2 < 1$ and the FWHM has its smallest value. Simultaneous with the minimum in FWHM when $\beta L = 2.6$, R is a maximum. Thus, when P_{Xe} is de-

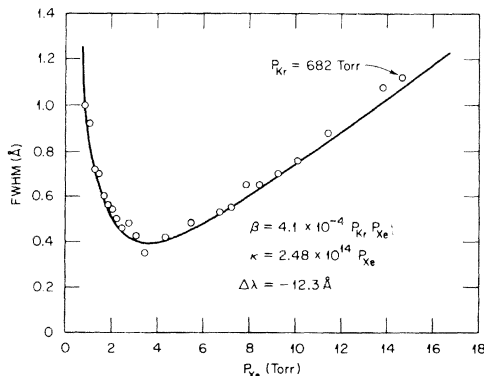


FIG. 6. Width of the phase-matched ionization signal vs P_{Xe} for Xe-Kr mixtures and $\Delta\lambda = -1.23$ nm relative to the $6s$ ($J=1$) resonance.

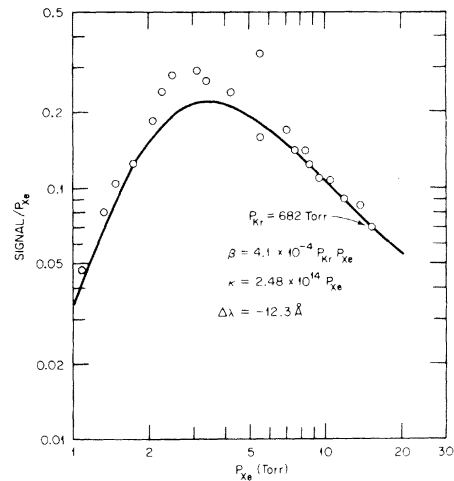


FIG. 7. Ratio of the phase-matched ionization signal to the three-photon resonance signal vs P_{Xe} for a Xe-Kr mixture and $\Delta\lambda = -1.23$ nm relative to the $6s$ ($J=1$) resonance.

creased or increased away from the point where $\beta L = 2.6$, FWHM increases and R decreases. In this limit the minimum observable FWHM for the phase-matched ionization signal is several times larger than 4.08σ , the width of the ionization signal in 3ω at three-photon resonance. The latter property makes it easy to identify situations where Eq. (7) applies. When $\Gamma_1 \gg Y_2$ and $\beta L > 5$, the FWHM $= 2\beta\Delta_m^2/\kappa$, as described earlier.

In the region described by Eq. (7), $K(3\omega, T)$ is easily determined from data on the FWHM which is increasing linearly with P_{Xe} . The determination of $K(3\omega, T)$ from FWHM data at high pressure is much more accurate than a value based on $\beta L \approx 2.6$ at the minimum of FWHM vs P_{Xe} . Figure 1 shows typical ionization signals observed when Xe at $P_{Xe} = 1.44$ Torr is mixed with various pressures of Kr to achieve phase matching at different wavelengths. The three-photon resonance signal with $F \approx 0.5$ has been divided into the measured peak heights to give a normalized peak height as tabulated in the figure. Since both $K(3\omega, T)$ and $\gamma_I(\Delta\lambda)$ vary from point to point, such data are difficult to interpret. Much more can be learned by fixing P_{Xe}/P_B while changing P_{Xe} . In this way $K(3\omega, T)$ and $\gamma_I(\Delta\lambda)$ stay fixed as P_{Xe} is varied.

In Fig. 2 the cell (described earlier) was initially filled with $P_{Xe} = 2.4$ Torr and $P_{Ar} = 128.5$ Torr. The laser was scanned for $386.0 \leq \lambda \leq 389.0$ with about 70% of the incident light reflected back through the cell. Ionization peaks were observed at 387.6 and 388.68 nm with the peak at 388.68 nm having a width (i.e., FWHM) of 0.013 nm. The 388.68-nm peak corresponds to three-photon resonance between the ground state and the $6s'$ ($J=1$)

state of Xe. With Xe-Ar mixtures and $P_{Xe}/P_{Ar} \ll 1$, calculations based on the oscillator strength of resonance and estimates of the index of refraction of Ar predict that phase matching should occur for a $\Delta\lambda$ (nm) $\simeq -(50 \pm 5)P_{Xe}/P_{Ar}$ detuning of the laser relative to three-photon resonance.

After the original mixture was introduced and measurements of FWHM for the phase-matched signal at 387.6 nm and the fraction of phase matched to resonance signals were made, the cell was pumped down to lower pressures and the measurements repeated. Within an accuracy of 0.01 nm the position of both peaks remained fixed. Figure 2 shows FWHM vs P_{Xe} at three experimental points. The solid curve was calculated using Eq. (4) with $\sigma = 1.2 \times 10^{11}$ /sec, $F_{01} = 0.19$, and corresponding to the observed position of phase matching. In this pressure range FWHM was very insensitive to assumptions about β . In Fig. 3 the ratio of phase-matched peak signal to resonance signal is plotted versus P_{Xe} . The observed plot implies $R \propto P_{Xe}^3$ which is consistent with $Y_2 \ll 1$ and our assumptions about the ionization mechanism.

In Figs. 4 and 5 the cell was originally filled with $P_{Xe} = 6.8$ Torr and $P_{Ar} = 799$ Torr. The laser was scanned between 439.0 and 441.0 nm and ionization peaks were observed at 439.62 and 440.88 nm. The 440.88-nm line has FWHM equal to 0.013 nm, and its position indicates that it corresponds to the three-photon resonance. Here about 50% of the incident beam is reflected back through the cell. When the reflected beam is blocked, no signal can be seen at 440.88 nm and the noise level is ~ 200 times less than the original signal. The cell was pumped down and measurements of the width and amplitude of the signal at 439.62 nm were made to give FWHM vs P_{Xe} and observed peak ratios. Again, $\Delta\lambda$ remains fixed to an accuracy of 0.01 nm, indicating $P_{Xe}/P_{Ar} = \text{const}$. The smooth curves in Figs. 4 and 5 are calculated from theory with $\sigma = 9.3 \times 10^{10}$ /sec, $F_{01} = 0.285$, $K(3\omega, T) = 1.3 \times 10^{-4}P_{Xe}P_{Ar}$, and with Δ_m corresponding to $\Delta\lambda$ (nm) = -1.26 nm. The theoretical curve for R was multiplied by a constant factor to achieve agreement with experiment at the highest pressure. This compensates for $[\gamma_I(\Delta\lambda)]/\gamma_I(0)$ which is certainly not unity in this region. From the magnitude of constant factors required in R near the $6s$ ($J=1$) resonance, $\gamma_I(\Delta\lambda)/\gamma_I(0)$ is near unity at small $\Delta\lambda$, but by

$\Delta\lambda \simeq -1$ nm it is ~ 3 .

In Figs. 6 and 7 the cell is initially filled with $P_{Xe} = 14.6$ Torr and $P_{Kr} = 682$ Torr. Here we observe $\Delta\lambda$ (nm) = -1.23 nm and, as usual, $\Delta\lambda$ stays fixed as the total pressure is pumped down. Figures 5 and 6 are of particular interest since in this situation $\beta = KP_{Xe}P_{Kr}$ and measurements by Castex¹¹ suggest $K \simeq 4 \times 10^{-4}$ with pressures in Torr and β in cm^{-1} .

The smooth curves are from theory with $\sigma = 9.3 \times 10^{10}$ /sec, $F_{01} = 0.285$, β (cm^{-1}) = $4.1 \times 10^{-4}P_{Kr}P_{Xe}$, and Δ_m corresponds to the observed separation of the peaks. For $P_{Xe} > 8$ Torr the observed line shapes at phase matching were Lorentzian. The theoretical curve for R was again multiplied by a constant factor to achieve agreement at $P_{Xe} = 10$ Torr.

In Fig. 7 the ratio signal starts to decrease at high pressure. The decrease is due to dimer absorption. In Figs. 6 and 7, Eq. (8) applies for $P_{Xe} > 8$ Torr and here $\text{FWHM} = 2\Delta_m^2\beta/\kappa$. Both R and FWHM are sensitive indicators of β at high pressures.

IV. CONCLUSIONS

In the cases shown here, as well as in many other situations, we have observed excellent agreement between theory and experiment. The agreement is so good that if F_{01} , β , and Δ_m had not been known, they could have been determined with high precision by measuring Δ_m and fitting the pressure dependences of R and FWHM. We have observed the limit of Eq. (6b) for Xe-Kr mixtures, with phase matching occurring at laser wavelengths of 387.67 nm and $P_{Xe} < 15$ Torr. Indeed, as predicted, the linewidth of the ionization signal at the phase-matched region was identical to the width observed at three-photon resonance.

ACKNOWLEDGMENTS

This research was sponsored by the Office of Health and Environmental Research, U.S. Department of Energy under Contract No. W-7405-eng-26 with the Union-Carbide Corporation. The work of W.R.F. was performed under appointment to the Laboratory Graduate Participation Program administered by the Oak Ridge Associated Universities for the Department of Energy.

¹K. Aaron and P. M. Johnson, J. Chem. Phys. **67**, 5099 (1977).

²J. C. Miller, R. N. Compton, M. G. Payne, and W. R. Garrett, Phys. Rev. Lett. **45**, 114 (1980); R. N. Comp-

ton, J. C. Miller, A. E. Carter, and P. Kruit, Chem. Phys. Lett. **71**, 87 (1980); J. C. Miller and R. N. Compton, Phys. Rev. A **25**, 2056 (1982).

³M. G. Payne, W. R. Garrett, and H. C. Baker, Chem.

- Phys. Lett. 75, 468 (1980).
- ⁴M. G. Payne and W. R. Garrett, Phys. Rev. A 26, 356 (1982).
- ⁵M. G. Payne and W. R. Garrett (unpublished).
- ⁶M. G. Payne, W. R. Garrett, and W. R. Ferrell (unpublished).
- ⁷J. H. Glowina and R. K. Sander, Phys. Rev. Lett. 49, 21 (1982).
- ⁸D. Jackson and J. J. Wynne (private communication); Phys. Rev. Lett. 49, 543 (1982).
- ⁹W. R. Ferrell, W. R. Garrett, M. G. Payne, and John C. Miller (unpublished).
- ¹⁰See, for instance, G. C. Bjorklund, IEEE J. Quantum Electron. QE-11, 287 (1975).
- ¹¹M. C. Castex, J. Chem. Phys. 66, 3854 (1977).